AD-786 847

STUDIES IN OPTICS

Douglas C. Sinclair, et al

Rochester University

Prepared for:

Advanced Research Projects Agency
Air Force Avionics Laboratory

June 1974

AD 786 847

DOCUMENT CONTROL DATA - R & D

(Security classification of title, body of abstract and indexing annotation must be entered when the overall report is classified)

1 ORIGINATING ACTIVITY (Corporate author)	2a. REPORT SECURITY CLASSIFICATION
The Institute of Optics University of Rochester Rochester, New York 14627	unclassified
	2b. GROUP

3 REPORT TITLE

STUDIES IN OPTICS

4 DESCRIPTIVE NOTES *(Type of report and inclusive dates)*
Technical.   1970 Feb 13 to 1973 Dec 15.

5 AUTHOR(S) *(First name, middle initial, last name)*

Douglas C. Sinclair; Michael Hercher; Brian J. Thompson

6 REPORT DATE	7a. TOTAL NO OF PAGES	7b. NO. OF REFS
June 1974	65	7
8a. CONTRACT OR GRANT NO. F33615-70-C-1451-P00006 b. PROJECT NO. 0745	9a. ORIGINATOR'S REPORT NUMBER(S) none	
c.	9b. OTHER REPORT NO(S) *(Any other numbers that may be assigned this report)*	
d.	AFAL-TR-74-177	

10. DISTRIBUTION STATEMENT

Approved for public release; distribution unlimited.

11. SUPPLEMENTARY NOTES	12. SPONSORING MILITARY ACTIVITY
	Advanced Research Projects Agency, Air Force Avionics Laboratory, Air Force Systems Command, Wright-Patterson AFB, Ohio

13. ABSTRACT

The studies covered in this report are the design of optical frequency shifters for AC interferometry (Section II) and the production and assessment of corrector plates used to optically compensate for distortions in laser beams (Section III).

Section II describes efforts to work out an electro-optical system for producing Doppler frequency shifts in laser beams. Earlier efforts to build practical AC interferometers ran into difficulties with the frequency shifters required: vibrating mirrors and other mechanically moving frequency shifters had to be discarded. Early experiments with electro-optical frequency shifters had practical difficulties in obtaining high enough spectral purity in the output beam. These difficulties have now been overcome.

Section III describes the design, fabrication, and testing of a correction plate for removing distortions in a laser beam. The work consisted of 1) measuring the deformation to be corrected, 2) digitizing the deformation information, 3) preparing a paper tape to control an optical milling machine, 4) machining a scaled-up correction plate, and 5) using the correction plate with the appropriate index-matching fluid to attempt to correct the original deformation. The pilot experiment clearly demonstrated the feasibility of this approach to correcting arbitrary wavefront deformations. With our current capability we could easily reduce wavefront distortions of as much as 50 wavelengths to less than one wavelength. Our approach would be particularly well-suited to the correction of large numbers of optical components, since all required operations can be done relatively inexpensively and routinely after the initial set-up.

DD FORM 1473
1 NOV 65

i.

14 KEY WORDS	LINK A		LINK B		LINK C	
	ROLE	WT	ROLE	WT	ROLE	WT
Optics						
Systems, optical						
Lasers						
Interferometry						
Interferometers						
Electro-optics						
Fabrication						

1a

STUDIES IN OPTICS

Michael Hercher
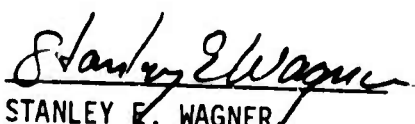Douglas C. Sinclair
Brian J. Thompson

ib
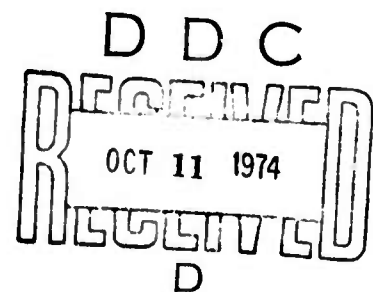
FOREWORD

These studies were conducted by members of The Institute of Optics, The University of Rochester, Rochester, New York 14627, under the sponsorship of the Advanced Research Projects Agency, Project No. 745, Contract F33615-70-C-1451. The Air Force Program monitor was Dr. Michael Heil (AFAL/TEO), Air Force Avionics Laboratory, Air Force Systems Command, Wright-Patterson Air Force Base, Ohio 45433. The studies reported here are a continuation of Contract F33615-70-C-1451. Previous results have been reported in Technical Reports AFAL-TR-73-112, "Studies in Optics", April 1973, and AFAL-TR-71-346, "Studies in Optics", March 1972.

Portions of the present study were performed by Institute of Optics graduate students Jean Louis Meyzonnette and Gih-Horng Chen.

Inclusive dates of the project are 13 February 1970 to 15 December 1973. This technical report was submitted by the authors on 27 May 1974 and approved as of 5 August 1974.

This technical report has been reviewed and is approved for publication.

MICHAEL M. HEIL
Project Engineer

STANLEY E. WAGNER
Act'g Chief
Electro-Optics Device Branch

ii

ABSTRACT

The studies covered in this report are the design of optical frequency shifters for AC interferometry (Section II) and the production and assessment of corrector plates used to optically compensate for distortions in laser beams (Section III).

Section II describes efforts to work out an electro-optical system for producing Doppler frequency shifts in laser beams. Earlier efforts to build practical AC interferometers ran into difficulties with the frequency shifters required: vibrating mirrors and other mechanically moving frequency shifters had to be discarded. Early experiments with electro-optical frequency shifters had practical difficulties in obtaining high enough spectral purity in the output beam. These difficulties have now been overcome.

Section III describes the design, fabrication, and testing of a correction plate for removing distortions in a laser beam. The work consisted of 1) measuring the deformation to be corrected, 2) digitizing the deformation information, 3) preparing a paper tape to control an optical milling machine, 4) machining a scaled-up correction

plate, and 5) using the correction plate with the appropriate index-matching fluid to attempt to correct the original deformation. The pilot experiment clearly demonstrated the feasibility of this approach to correcting arbitrary wavefront deformations. With our current capability we could easily reduce wavefront distortions of as much as 50 wavelengths to less than one wavelength. Our approach would be particularly well-suited to the correction of large numbers of optical components, since all required operations can be done relatively inexpensively and routinely after the initial set-up.

TABLE OF CONTENTS

LIST OF ILLUSTRATIONS

I. REPORT SUMMARY

The work described in this report is a continuation
of earlier studies under Contract F33615-70-C-1451 and
covers two principal areas of interest: design of an
electro-optical frequency shifter for use in AC interfero-
metry, and the production and testing of a scaled correction
plate for optical correction of beam divergence in crystal
and glass laser rods.

Design of an Electro-Optical Frequency Shifter

We found during the course of our experimental in-
vestigation that a primary problem in building practical
AC interferometers was obtaining frequency shifters that
could be used to produce the local oscillator beams needed
for them. Most of our early experiments utilized vibrating
mirrors to produce frequency shifts in laser beams by Doppler
methods (a technique called serrodyning). We found, however,
that it was difficult to obtain reliable operation from such
devices, and that more sophisticated frequency shifters were
needed. At the same time, the bandwidth requirements of our
system prohibited the use of mechanically moving frequency
shifters, so we resorted to an electro-optical system.

In our early experiments with an electro-optical frequency
shifter, we found that the spectral purity of the output beam

1

from the frequency shifter was not sufficiently high to make it useful for an AC interferometer. We therefore set about a series of experiments to determine the effect of various modulator characteristics on the spectral purity of a frequency shifted output beam. Both single-pass and double-pass configurations were tried. The output beam had greater spectral purity in the double-pass configuration.

A Method of Optically Correcting Crystal and Glass Laser Rods

The beam distortion to be corrected is determined by obtaining an interferogram of a wavefront which has been distorted by passage through the laser rod responsible for the distortion. This interferogram is essentially a contour map of the distorted wavefront, and also a contour map of the desired optical thickness of the finished correction plate. The plate is made to conform to the interferogram contours except that high spots on the interferogram become low spots on the correction plate, and vice versa. If the original beam is passed through this correction plate, a distortion-free beam should result.

For accuracy in machine contouring of the plate surface, we enlarge the distortion by a scale factor M. Contouring is done semi-automatically by an optical milling machine controlled in depth-of-cut by a paper tape generated using

data taken from a photograph of the interferogram. The contoured plate must then be scaled back down to the proper magnitude for use. This is done by immersing it in a fluid of refractive index nearly matching the index of the plate. An index mismatch of Δn produces a scale factor $M = 1/\Delta n$. The near-matching technique also does away with the necessity for optically polishing the correction plate, since the surface roughness is scaled down by the same factor M.

The final steps in the study involve immersion of the completed correction plate in the near-matching index fluid and testing of the original beam for absence of distortion. The correction plate proved to be successful. When the plate was inserted into the beam, a marked improvement in the quality of the transmitted wavefront was obtained: 20 fringes of deformation in the uncorrected beam were reduced to only a few fringes. Even better results can be achieved with a more refined version of the same basic technique.

II. DESIGN OF OPTICAL FREQUENCY SHIFTERS

FOR AC INTERFEROMETRY

1. Single Sideband Suppressed Carrier Modulation of Light by Electro-Optic Techniques

The method of detecting a signal by mixing it with a reference signal of different frequency (heterodyning) has been widely used in the domain of radio communications. Since the advent of lasers, the properties of heterodyne detection have been applied to optical communications as well, and seem to have promising applications in such areas as Laser Doppler Velocimetry and fringe-counting interferometry, where the heterodyne signal is easily related to the speed of the moving particles or the displacement of an object under test.

The Doppler shifting of optical frequencies can be produced by several means. Most of those now in use are mechanical: for example, the linear translation of a mirror, linear rotation or translation of a grating, rotation of a half wave plate, etc. Other methods are electromagnetic in nature, using the change in refractive index of the medium due to magnetic, acoustic or electric fields. Although the mechanical means have the advantage of ease in alignment and simplicity, their use is limited by their very low bandwidth, especially in interfe ometric applications where they can upset the experiment by the vibrations they generate. Magneto optic methods (Zeeman effect) require rather high magnetic fields, because of

the smallness of the Verdet constant for most media. Acousto-optic frequency shifting (Bragg diffraction) usually alters the direction of the beam, which makes it very useful for constructing beam deflectors or holographic memory readers, but unfit for the interferometric applications we are mainly interested in.

Hence, we will limit our attention to electro-optic frequency shifters, comparing them in efficiency, power requirements, ease of adjustment, etc.

2. Theory of Electro-Optic Frequency Shifting

The electro-optic modulation of light makes use of
the fact that two different polarizations of light exper-
ience two slightly different indices of refraction when
going through an electro-optic crystal upon which some
voltage is applied. By modulating this voltage, one
changes the optical path through the crystal at will, and,
hence, one modifies the instantaneous frequency of the
output light.

$$\underset{\mathscr{E}=\mathscr{E}_o e^{i(\omega_o t - k_o z)}}{\overset{input\ light}{\longrightarrow}} \boxed{E\text{-}O\ CRYSTAL} \underset{\mathscr{E}=\mathscr{E}_o e^{i(\omega_o t - k(t)z)}}{\overset{output\ light}{\longrightarrow}}$$

$$\uparrow$$

$$Voltage\ \ V = V(t)$$
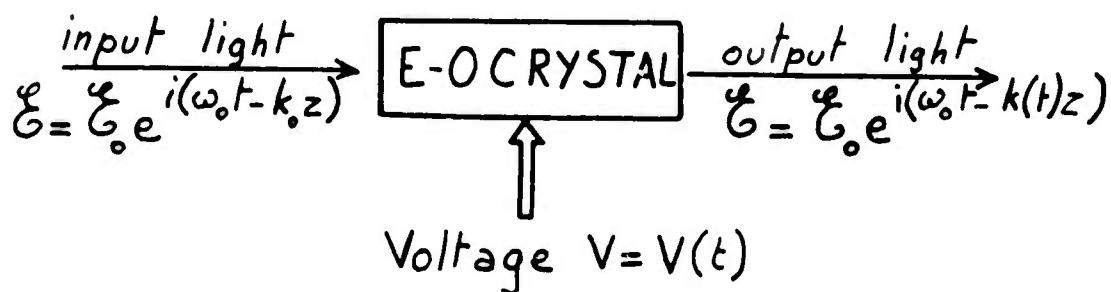
The frequency of the output light depends on the
modulating function $V(t)$, and in the following pages we
will investigate several of the voltage excitations that
must be used in order to obtain a constant shift in the
frequency of the input light.

Without going too far back into the general prop-
erties of electro-optic crystals, we recall that the
dielectric constant of a homogeneous, nonconducting and
anisotropic medium is a symmetric tensor, so that it is
made up of 6 independent components. The structure of

7

an anisotropic medium allows two monochromatic plane waves
with two different polarizations and two different veloc-
ities to propagate in any given direction, and both the
velocities and the directions of polarization can be easily
found from the index ellipsoid of the medium built from
the dielectric tensor:

$$\frac{x^2}{n_1^2} + \frac{y^2}{n_2^2} + \frac{z^2}{n_3^2} + \frac{2yz}{n_4^2} + \frac{2zx}{n_5^2} + \frac{2xy}{n_6^2} = 1$$

where the standard notation is used:

$$\varepsilon_{kl} = \varepsilon_{lk} = n_{lk}^2 = n_i^2 \quad and:$$

l	k	i
1	1	1
2	2	2
3	3	3
2	3	4
1	3	5
1	2	6

The two planes of polarization which are allowed
in the crystal to an incoming beam are obtained by consi-
dering the intersection of the index ellipsoid with the
plane perpendicular to the direction of propagation of
the beam: if it is an ellipse, the allowed polarizations
are parallel to the main axes of the ellipse and the

8

corresponding indices of refraction are half the length
of these axes. If the intersection is a circle, then the
crystal is isotropic for that particular direction of
propagation. When the crystal is subjected to an electric
field, the die'ectric constant, and hence, the index ellip-
soid undergo a change such that:

$$\left(\frac{1}{n_i^2}\right)_{\substack{with \\ field}} = \left(\frac{1}{n_i^2}\right)_{\substack{without \\ field}} + \sum_{j=1}^{3} r_{ij} E_j$$

where the E_j's are the three components of the field on
the x, y, z axes.

Usually, for most modulation purposes, the crystal
is cut in such a way that when no voltage is applied, the
crystal is isotropic for the incoming light. The setting
of an electric field makes the crystal anisotropic, the
directions of the fast and slow axes depending on the di-
rection of the electric field and the symmetry of the
crystal. The retardation introduced between the two
polarizations allowed to propagate through the crystal
is simply:

$$r_{xy} = \frac{2\pi}{\lambda} d\left(n_x - n_y\right)$$

where d is the thickness of the crystal. The crystal acts

9

then as an r-wave retarder, where the retardation r is proportional to the applied field (linear Pockels effect).

A. Case of One Crystal

1. Transverse field.

The effect of a rotating r-wave plate upon a circularly polarized beam of light is described by the Jones Calculus. The matrix corresponding to an r-wave plate, whose axes are at angle α with the x-y axes is the following:

$$T_{r\text{-}wave} = \begin{pmatrix} e^{-i\pi r}\cos^2\alpha + e^{i\pi r}\sin^2\alpha & \left(e^{-i\pi r}-e^{i\pi r}\right)\cos\alpha\sin\alpha \\ \left(e^{-i\pi r}-e^{i\pi r}\right)\sin\alpha\cos\alpha & e^{-i\pi r}\sin^2\alpha + e^{i\pi r}\cos^2\alpha \end{pmatrix}$$

The action of such a plate on a circularly polarized beam of light results in the following output beam:

$$\mathcal{E}_{IN} = \begin{pmatrix} 1 \\ i \end{pmatrix} e^{i\omega_o t} \implies \mathcal{E}_{OUT} = T\,\mathcal{E}_{IN}$$

$$\mathcal{E}_{OUT} = \sin\pi r \begin{pmatrix} 1 \\ -i \end{pmatrix} e^{i(\omega_o t + 2\alpha)} + \cos\pi r \begin{pmatrix} 1 \\ i \end{pmatrix} e^{i\omega_o t}$$

Hence, if we set the r-wave plate in a uniform rotation, the output light is made up of two components: one,

with amplitude cosπr is of the same frequency and state
of polarization as the input light, and the other one,
with amplitude sinπr, is shifted in frequency by twice
the frequency of rotation of the plate, and has polari-
zation orthogonal to that of the input light. If the
plate in use is a half-wave plate, a left circular beam
of light is totally transformed into a right circularly
polarized beam, up or down shifted in frequency (depen-
ding upon whether the rotation of the plate is in the
same or opposite direction as the direction of polari-
zation of the incoming light).

This method of a rotating half-wave plate has been
used for phase measurements in interferometry[1] and micros-
copy[2]. However, its range is limited to frequencies up
to several hundred Hertz, the mechanical rotation may
introduce vibrations or turbulence in the interferometric
set-up, and care must be taken to compensate for a
possible uneven thickness of the plate, which would gen-
erate a supplementary phase modulation of the beam.

It has been shown theoretically and experimentally[3,4,5]
that the same effect can be obtained without any mechan-
ical rotation, by applying a rotating transverse electric
field to crystals of cubic symmetry, and of point group
$\overline{4}3m$, when light is being propagated along the threefold
axis. When no voltage is applied, the crystal is isotro-
pic, and when a transverse field is on, the amount of

birefringence induced in the crystal depends only upon the magnitude of the field, but not upon its direction, although the direction of the axes of birefringence are related to the direction of the field, as it can be shown in the next lines, taken from Kamikow and Turner's article[5]:

From the symmetry of a cubic, $\bar{4}3m$ crystal, it follows that the electro-optic tensor of such a crystal (for example, zinc sulfide, or lithium niobate) is such that:

$$r_{12} = r_{61} = -r_{22}$$

$$r_{21} = r_{62} = -r_{11}$$

When the transverse electric field $\underline{E}(E_x, E_y)$ is applied perpendicularly to the direction of propagation of light, the equation of the index ellipsoid in the $z = 0$ plane becomes:

$$\left[\frac{1}{n_i^2} + \left(r_{11} E_x - r_{22} E_y\right)\right] x^2 + \left[\frac{1}{n_i^2} + \left(r_{22} E_y - r_{11} E_x\right)\right] y^2$$

$$+ 2\left[-r_{22} E_x - r_{11} E_y\right] xy = 1$$

After a suitable rotation of its axes, the equation of this ellipse becomes:

12

$$\left[\frac{1}{n_1^2} + \left(r_{11}^2 + r_{22}^2 \right)^{\frac{1}{2}} E \right] x^2 + \left[\frac{1}{n_1^2} - \left(r_{11}^2 + r_{22}^2 \right)^{\frac{1}{2}} E \right] y^2 = 1$$

where E is the amplitude of the electric field:

$$E_x = E \cos \phi$$

$$E_y = E \sin \phi$$

The angle between the principal axes of the ellipse and the x-y axes is:

$$\theta = -\frac{1}{2} \left[\phi + Arc \sin \frac{r_{22}}{\sqrt{r_{11}^2 + r_{22}^2}} \right]$$

Hence, as the transverse electric field is set into rotation, the axes of induced birefringence rotate twice as slowly, and the shift in the frequency of the optical beam is equal to the frequency of rotation of the electric field.

Experimentally, the transverse rotating field is obtained by feeding two pairs of orthogonal plane electrodes respectively with sine and cosine wave voltages. The method has been tried in the audio range with a zinc sulfide crystal, unfortunately of very poor optical quality[3], and with better results, at 110 MHz with lithium niobate[4].

13

2. Transverse or Longitudinal Excitation.

The effect equivalent to the linear translation of
a mirror to shift the frequency of the incoming beam may
be obtained by applying a linear voltage to electro-optic
crystals. This effect (called serrodyning) has been used
to shift the frequency of gaussian pulses[6] by synchro-
nizing laser pulses with the zero crossings of an applied
sinusoidal field. It can also be shown[7] that, when this
method is used with a quasimonochromatic input light, the
total energy of the output beam is found at the shifted
frequency if the saw tooth modulation is used and the
maximum voltage of the ramp is the half-wave voltage of
the crystal.

B. Case of Two Crystals

Instead of using the transverse electro-optic
effect or linear excitation, as in serrodyning, we in-
vestigate the possibilities of a longitudinal sine-wave
excitation, which allows the use of good optical quality
crystals of the KDP type. These crystals are quite strain
free, and do not become opaque after being exposed to U.V.
radiation as $LiNbO_3$ does. Because they absorb very little
light, the problem of heating is avoided. Since the ex-
citation is along the direction of propagation of light,
the principal axes of induced birefringence are no longer

14

determined by the direction of the electric field, but
by the symmetry of the crystal itself. Since no physical
rotation of the crystal is desirable, one has to use more
than one crystal along the path of light in order to
obtain the frequency shift of the incident light.

Consider the case of two Z-cut crystals in the longi-
tudinal mode, so that their optic axis is parallel to the
direction of propagation of the incident beam and they
are isotropic when no voltage is applied. Their princi-
pal axes are at an angle α with each other. The voltages
are sine wave functions, and we suppose that the incoming
light is elliptically polarized:

$$\begin{cases} V_1 = V_0 \cos \omega_m t \\ V_2 = V_0 \cos(\omega_m t + \varphi) \end{cases} \qquad \text{and} \qquad E_{in} = \begin{pmatrix} E_{ox} \\ E_{oy} e^{i\phi} \end{pmatrix} e^{i\omega_o t}$$

When a voltage is applied longitudinally on a
crystal, the index ellipsoid is changed from:

$$\frac{x^2 + y^2}{n_o^2} + \frac{z^2}{n_e^2} = 1$$

to:

$$\frac{x^2}{n_1^2} + \frac{y^2}{n_2^2} + 2xy\, r_{63}\, E_z + \frac{z^2}{n_e^2} = 1$$

15

The changes in index of refraction along the induced fast and slow axes are then:

$$\frac{1}{\eta_1^2} = \frac{1}{\eta_o^2} + r_{63} E_z$$

$$\frac{1}{n_2^2} = \frac{1}{n_o^2} - r_{63} E_z$$

and the retardation r between the two components of an optical field along these axes is:

$$\delta = 2\pi r = \frac{2\pi}{\lambda}\left(\Delta n_x - \Delta n_y\right)d$$

Since $\Delta n = \frac{n^3}{2}\Delta\left(\frac{1}{n^2}\right)$, the retardation is then:

$$\delta = 2\pi r = \frac{2\pi}{\lambda} n^3 r_{63} E_z d = \frac{2\pi}{\lambda} n^3 r_{63} V$$

Knowing the characteristics of the input light, we deduce easily the components of the output light by use of the transfer matrices of the two crystals:

$$E_{out} = T_2 T_1 E_{in}$$

16

$$E_x = \left[E_{ox} e^{i\frac{\delta_1}{2}\cos\omega_m t} \cos\alpha + E_{oy} e^{-i\frac{\delta_1}{2}\cos\omega_m t + i\phi} \sin\alpha \right] e^{i\frac{\delta_2}{2}\cos(\omega_m t+\varphi)}$$

$$E_y = \left[-E_{ox} e^{i\frac{\delta_1}{2}\cos\omega_m t} \sin\alpha + E_{oy} e^{-i\frac{\delta_1}{2}\cos\omega_m t + i\phi} \cos\alpha \right] e^{-i\frac{\delta_2}{2}\cos(\omega_m t+\varphi)}$$

where δ_1, and δ_2 are the maximum retardations induced respectively in the first and second crystals, and are directly proportional to the maximum voltages applied to the crystals, as seen from the relation between δ and V, above.

From the general expression giving the components of the output light, as stated above, we determine which values of the parameters (i.e. voltage phase shift, angle between the principal axes of the two crystals, voltage amplitude) maximize the output energy in the desired sideband. We consider that the incident light is circularly polarized, and that the voltages applied to both crystals have the same amplitude. Then, the output can be written as

$$E_x = e^{i\frac{\delta}{2}\left[\cos\omega_m t + \cos(\omega_m t+\varphi)\right]} \cos\alpha - i e^{-i\frac{\delta}{2}\left[\cos\omega_m t - \cos(\omega_m t+\varphi)\right]} \sin\alpha$$

$$E_y = -e^{i\frac{\delta}{2}\left[\cos\omega_m t - \cos(\omega_m t+\varphi)\right]} \sin\alpha - i e^{-i\frac{\delta}{2}\left[\cos\omega_m t + \cos(\omega_m t+\varphi)\right]} \cos\alpha$$

The spectral content of the output depends only upon δ, ϕ and α, and the following graphs describe the behavior of the first harmonics in the output for increasing values of the induced retardation δ, with respect to the two other parameters. An analysis of Figs. 1 and 2 shows that complete elimination of the lower sideband is obtained when the electrical voltages applied to the crystals are in quadrature ($\phi = \frac{\pi}{2}$) and the output of the desired sideband is maximized when the principal axes of the crystals are at 45° with respect to each other. These conclusions are true whatever the maximum induced retardation is.

One may note that these results are reversed, that is, the upper sideband is totally eliminated and the output of the lower sideband is maximized if the two crystals are rotated by $\frac{3\pi}{4}$ instead of $\frac{\pi}{4}$, or if the phase difference between the two voltages has its sign changed. The lower sideband can also be maximized if right circularly polarized light (instead of left circularly polarized) is incident upon the original set-up. Hence, one may eliminate at will one of the two sidebands and maximize the other one by one of the following changes:

- right circular polarization $\longrightarrow$ left circular
- $\varphi = \frac{\pi}{2}$ $\longrightarrow$ $\varphi = -\frac{\pi}{2}$
- $\alpha = \frac{\pi}{4}$ $\longrightarrow$ $\alpha = \frac{3\pi}{4}$

18

Relative amplitude of harmonics
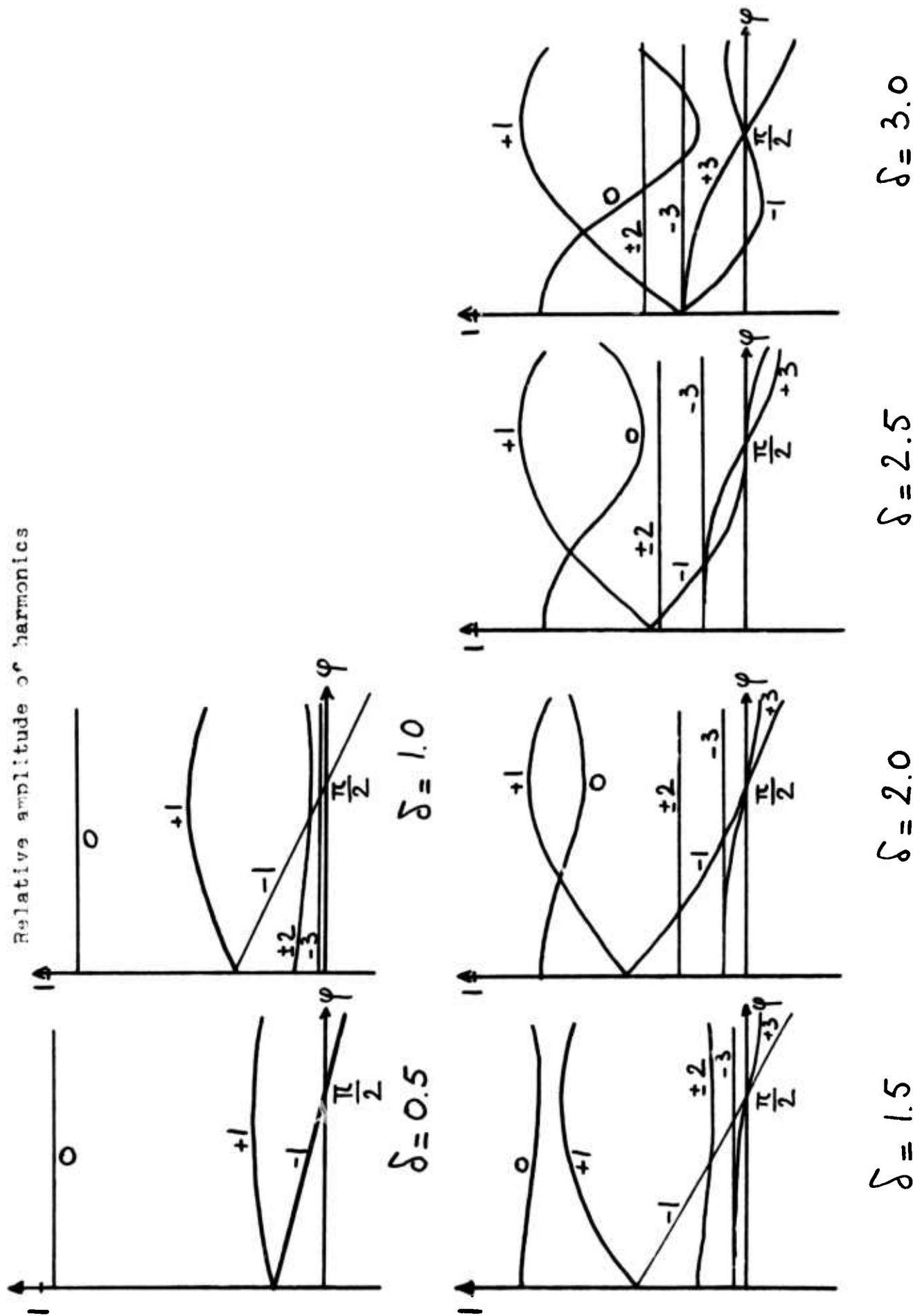
Fig. 1. Spectral content of the output versus the phase shift φ between the voltages applied.
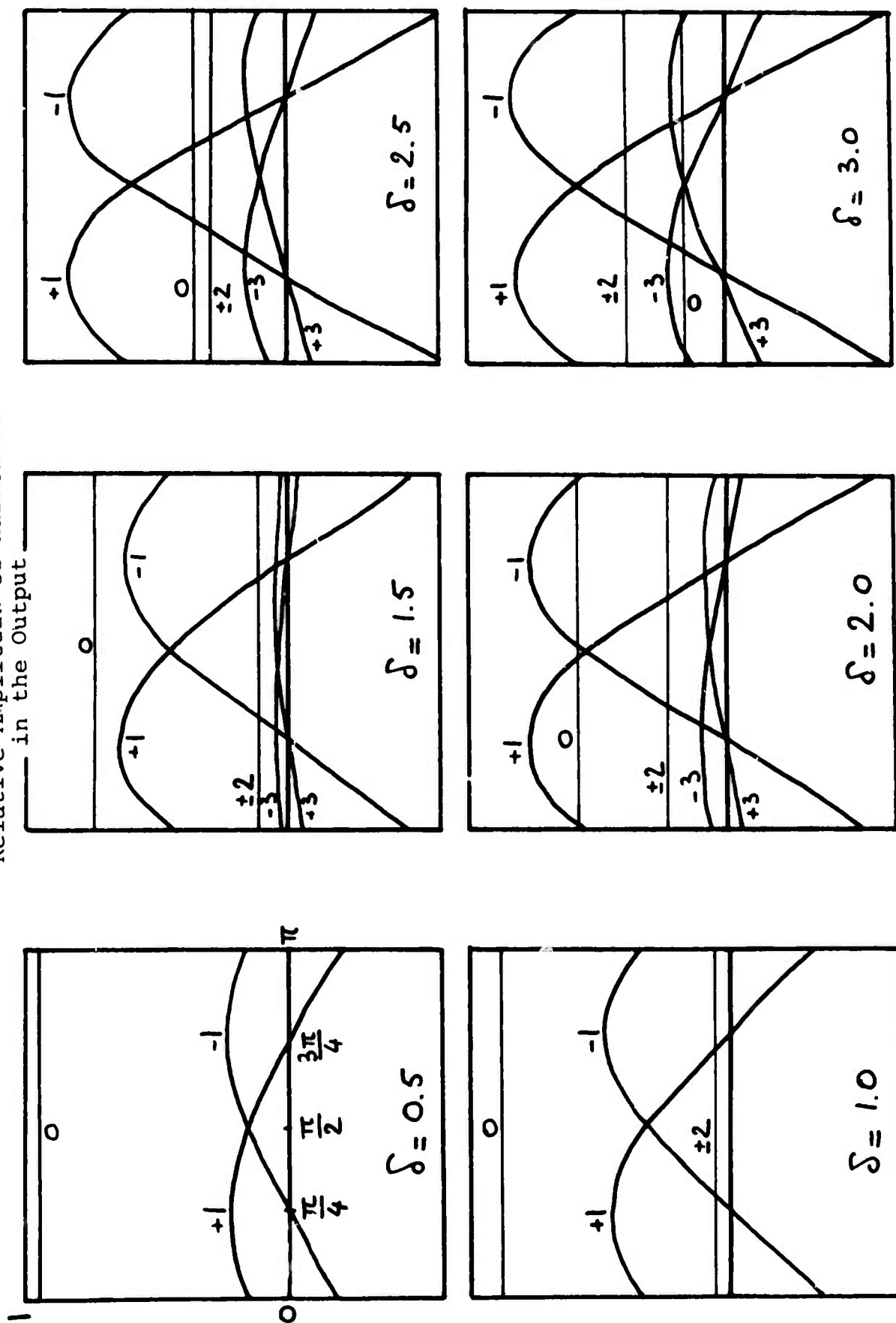
19

Fig. 2.
Spectral Content of the Output with respect to the angle α between the principal axes of the Crystals

20

Let the incident light be circularly polarized, the
voltages applied to the crystals be of equal amplitude
and in quadrature, and the crystals oriented in such a
way that their birefringent axes are at 45 degrees with
respect to each other. Then the Jones vector correspon-
ding to the output light is:

$$
E_{out} = \begin{cases}
E_x = \dfrac{\sqrt{2}}{2}\, E_o \left[e^{\,i\frac{\delta}{2}\left[\cos\omega_m t + \cos\left(\omega_m t + \frac{\pi}{2}\right)\right]} \right. \\
\qquad\qquad \left. + i\, e^{\,i\frac{\delta}{2}\left[\cos\left(\omega_m t + \frac{\pi}{2}\right) - \cos\omega_m t\right]} \right] e^{\,i\omega_o t} \\[2em]
E_\gamma = \dfrac{\sqrt{2}}{2}\, E_o \left[-e^{\,i\frac{\delta}{2}\left[\cos\omega_m t - \cos\left(\omega_m t + \frac{\pi}{2}\right)\right]} \right. \\
\qquad\qquad \left. + i\, e^{\,-i\frac{\delta}{2}\left[\cos\omega_m t + \cos\left(\omega_m t + \frac{\pi}{2}\right)\right]} \right] e^{\,i\omega_o t}
\end{cases}
$$

Using the following relations:

$$
e^{\,iz\cos\theta} = \sum_{-\infty}^{+\infty} i^{\,k} J_k(z)\, e^{\,ik\theta}
$$

$$
J_k(-z) = (-1)^{\,k} J_k(z)
$$

one finds that the components of the output light are:

$$E_x = \frac{\sqrt{2}}{2} E_o \, e^{i\omega_o t} \sum_{-\infty}^{+\infty} i^k J_k\left(\frac{\sqrt{2}}{2}\delta\right) e^{ik\left(\omega_m t + \frac{\pi}{4}\right)} \left[1 + (-1)^k e^{-i(k-1)\frac{\pi}{2}}\right]$$

$$E_y = i\frac{\sqrt{2}}{2} E_o \, e^{i\omega_o t} \sum_{-\infty}^{+\infty} (-1)^k i^k J_k\left(\frac{\sqrt{2}}{2}\delta\right) e^{ik\left(\omega_m t + \frac{\pi}{4}\right)} \left[1 + (-1)^k e^{-i(k-1)\frac{\pi}{2}}\right]$$

The output beam can then be decomposed into an infinite series of right and left circularly polarized harmonics, the even ones having the same state of polarization as the incident beam, the odd ones being orthogonal to it, and with intensities given by:

$$\frac{I_{2n}}{I_{incident}} = J_{2n}^2\left(\frac{\sqrt{2}}{2}\delta\right)$$

$$\frac{I_{4n+3}}{I_{in}} = 0$$

$$\frac{I_{4n+1}}{I_{in}} = 2 J_{4n+1}^2\left(\frac{\sqrt{2}}{2}\delta\right)$$

By letting the beam go through a circular polarizer, one eliminates all the even harmonics, and, since an electro-optic crystal is always operated with voltages no higher than its half-wave voltage, the first harmonic is always much larger than the other odd harmonics exiting from the circular polarizer, and to a first approximation, the incident energy of the beam at frequency ω_0 is transmitted

through the system after being shifted to the frequency
$(\omega_\bullet + \omega_m)$, with an efficiency $2 J_1^2 \left(\frac{\sqrt{2}}{2} \delta \right)$.

Experimentally, we have set up this type of electro-optic frequency shifter by using two potassium dideuterium phosphate cells (KD*P), whose half-wave voltage is about 1800V, because each is made of two crystals optically in series and electrically in parallel. In order to compare the output of the system to the input light, we insert it in a Mach Zehnder interferometer:
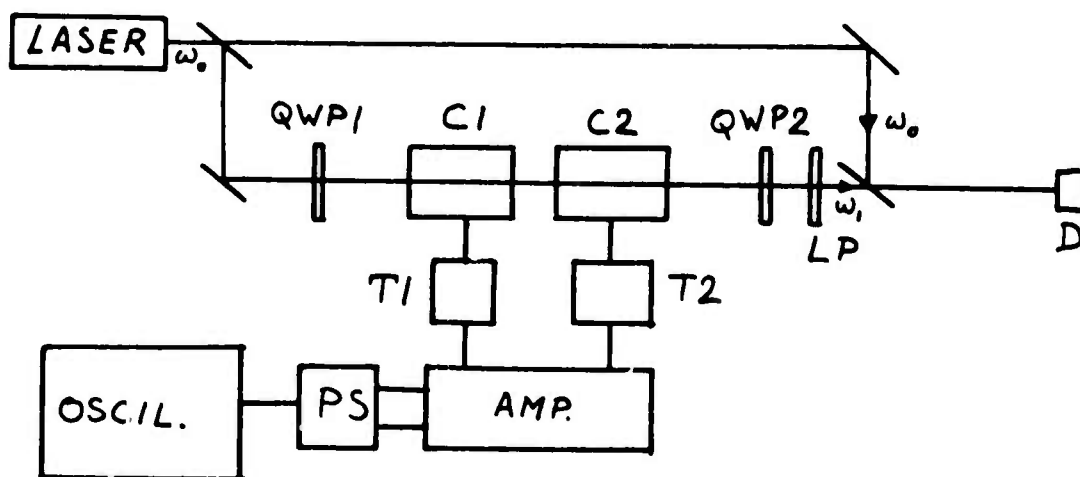
The linearly polarized light from the HeNe laser is made circularly polarized by means of the first quarter wave plate (QWP1). It then goes through the two electro-optic cells, C1 and C2, and the circular polarizer, made up of a quarter wave plate followed by a linear polarizer.

23

This final assembly brings complete extinction when no voltage is fed to the cells. This voltage is generated by meand of an oscillator, a phase shifter(PS) with two outputs whose relative phases can be adjusted, a 20 W stereo amplifier and two step-up transformers (T1 and T2).

In order to evaluate the performance of the actual set-up, we derive the output spectrum of the frequency shifter when some of the components are misaligned or present some defects, or when the input light is not circularly polarized.

For example, we show the computations involved in two cases, namely for misadjustment of the phase shift between the two voltages feeding the crystals, and for misalignment of a crystal.

In case the voltage phase shift is not $\frac{\pi}{2}$, we get the following expression for output components of the optical beam:

$$E_x = \frac{\sqrt{2}}{2} \left[e^{i\delta\cos\frac{\varphi}{2}\cos\left(\omega_m t + \frac{\varphi}{2}\right)} + i e^{-i\delta\sin\frac{\varphi}{2}\sin\left(\omega_m t + \frac{\varphi}{2}\right)} \right] e^{i\omega_o t}$$

$$E_\gamma = \frac{\sqrt{2}}{2} \left[-e^{i\delta\sin\frac{\varphi}{2}\sin\left(\omega_m t + \frac{\varphi}{2}\right)} + i e^{-i\delta\cos\frac{\varphi}{2}\cos\left(\omega_m t + \frac{\varphi}{2}\right)} \right] e^{i\omega_o t}$$

24

The spectral content of this output is again obtained through the "Golden Rule" of Bessel functions:

$$E_x = \frac{\sqrt{2}}{2} \sum_{-\infty}^{+\infty} i^k e^{ik\left(\omega_m t + \frac{\varphi}{2}\right)} \left[J_k\left(\delta \cos\frac{\varphi}{2}\right) + (-1)^k e^{-i(k-1)\frac{\pi}{2}} J_k\left(\delta \sin\frac{\varphi}{2}\right) \right] e^{i\omega_0 t}$$

$$E_y = \frac{\sqrt{2}}{2} \sum_{-\infty}^{+\infty} (-1)^k i^k \left[i J_k\left(\cos\frac{\varphi}{2}\right) - i^k J_k\left(\sin\frac{\varphi}{2}\right) \right] e^{i\omega_0 t} e^{ik\left(\omega_m t + \frac{\varphi}{2}\right)}$$

Hence, the major consequence of a misadjustment in the phase shift is the appearance of the (-1) order, with the following amplitude:

$$\mathcal{A}_{-1} = \frac{\sqrt{2}}{2} \left[J_1\left(\delta \cos\frac{\varphi}{2}\right) - J_1\left(\delta \sin\frac{\varphi}{2}\right) \right]$$

Instead of being completely suppressed, as is the case when $\varphi = \frac{\pi}{2}$, the residual (-1) order will be directly proportional to the phase error, and, since it has the same polarization as the (+1) order (upper sideband), it will go through the circular analyzer without being attenuated. The harmonic content of the output will also be made of the leakage from the lower sideband and all the (4n + 3) orders which do not exist when the two voltages are exactly in quadrature.

The leakage from the lower sideband, by far the most important, is then:

25

$$\mathscr{A}_{-1} = \frac{\sqrt{2}}{2}\left[J_1\left[\frac{\delta\sqrt{2}}{2}\left(1-\varepsilon\right)\right] - J_1\left[\frac{\delta\sqrt{2}}{2}\left(1+\varepsilon\right)\right]\right]$$

$$= \frac{\delta\varepsilon}{2} \quad \text{when} \quad \begin{cases} \delta < \dfrac{\pi}{2} \\ \varphi = \dfrac{\pi}{2} + \varepsilon \\ \varepsilon \ll 1 \end{cases}$$

Another case of great importance, one which may
degrade very easily the performance of the frequency
shifter, is a misalignment of the crystals. When the
beam is not propagating along the axis of the crystal,
the natural birefringence of the crystal as seen by the
incoming light may be of the same order of magnitude or
greater than the birefringence induced by the driving
voltage. The latter is always less than a half-wave if
one does not want to damage the crystal, while natural
birefringence caused by misalignment may be several wave-
lengths, depending on the thickness of the crystal and
the values of the ordinary and extraordinary indices. In
crystals like KDP, the difference between the two indices
is rather large, so that a very small displacement of the
axis is sufficient for a substantial birefringence to
appear. This problem does not exist in cubic-type crys-
tals like zinc sulfide, which are isotropic and may accept
a wide cone angle of incoming light without affecting its
state of polarization.

In order to determine the effect of crystal misalignment, we compute the amount of natural birefringence experienced by an incoming beam of light not propagating along the optic axis of the crystal. This is done by considering the intersection of the index ellipsoid with the plane normal to the direction of propagation of light. This intersection is usually an ellipse whose equation can be written with respect to the principal indices n_x, n_y, n_z of the crystal and the direction cosines α, β, γ of the incident light:

$$\begin{cases} \alpha x + \beta y + \gamma \delta = 0 \\ \dfrac{x^2}{\varepsilon_x} + \dfrac{y^2}{\varepsilon_y} + \dfrac{z^2}{\varepsilon_z} = 1 \end{cases}$$

After evaluating the lengths of the ellipse's main axes, one finds that the phase difference between the two linear components of light propagating through the crystal can be written as follows:

$$\delta \phi = \frac{2\pi}{\lambda} \frac{d}{\cos r} \left(n_z - n_x \right) \sin \theta_1 \sin \theta_2$$

where θ_1 and θ_2 are the angles between the wave normal and the two axes of the crystal. The additional phase difference, created by the fact that light is no longer propagating along the optic axis of the crystal, introduces

27

a set of harmonics which show up in the output of the
frequency shifter and degrade its spectral purity. It
is easy to see that when no voltage is applied on one of
the electro-optic crystals, the natural birefringence intro-
duced by it is:

$$\delta\phi = \frac{2\pi}{\lambda} \frac{d}{\cos r} \left(n_z - n_x\right) \sin^2 r$$

The leakage of other orders than the hoped-for side-
band is directly proportional to this phase shift, which
sets a maximum misalignment angle for both crystals if
a high spectral purity is to be obtained.

Since the electro-optic effect depends upon the length
of the crystals, it is doubled if the beam goes twice into
the crystals, for example, after reflection upon a mirror.
So, we have also tried the following configuration, with
double passage of light through the crystals:

28
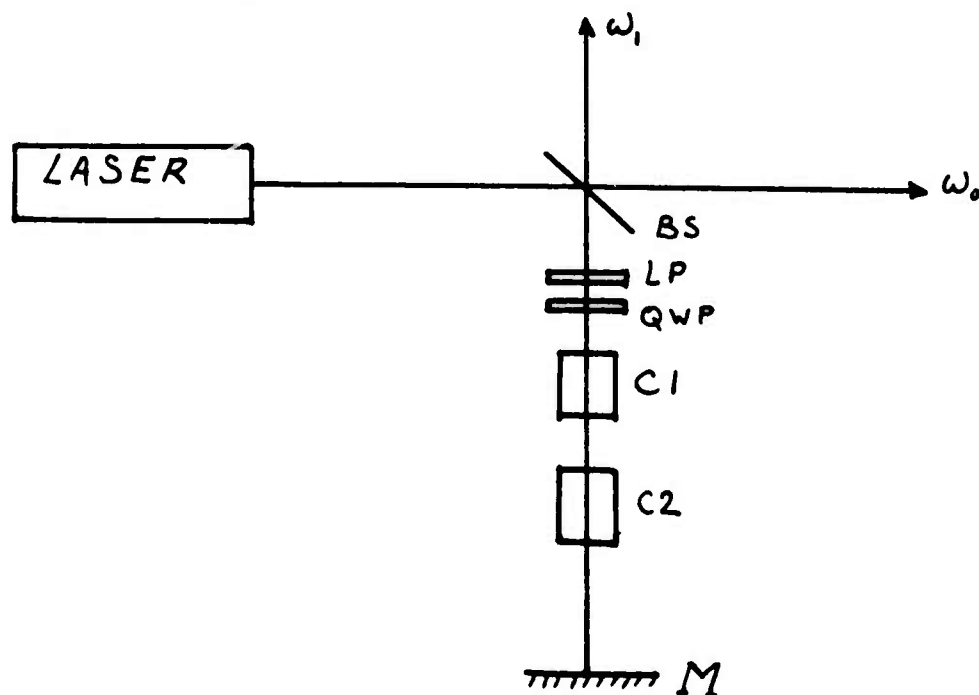
As before, the axes of the crystals are at 45° with respect to each other, the voltages are in quadrature, and, by applying Jones calculus to the beam of light on its way back, we find that the output light right before the circular analyser has the following components:

$$\mathcal{A}_{4n} = J_{4n}\left(\delta\sqrt{2}\right)$$

$$\mathcal{A}_{4n+2} = 0$$

$$\mathcal{A}_{2n+1} = \frac{\sqrt{2}}{2} J_{2n+1}\left(\delta\sqrt{2}\right) + (-1)^{n+1} J_{2n+1}\left(\delta\right)$$

All the odd harmonics go through the circular analyser without being attenuated, while the even ones are eliminated by it. The theoretical efficiency curves are plotted on p.30 as well as some experimental results. We can see that, contrary to the preceding single-pass set-up, the lower sideband is present in the output, but, for voltages lower than the quarter wave voltage, it is quite negligible, compared to the upper sideband, due to the linearity of the first-order Bessel function in that region. It is also seen that the efficiency of transforming the intensity from the original frequency to the upper sideband is twice the efficiency obtained with the single pass set-up, for low voltages, since then:
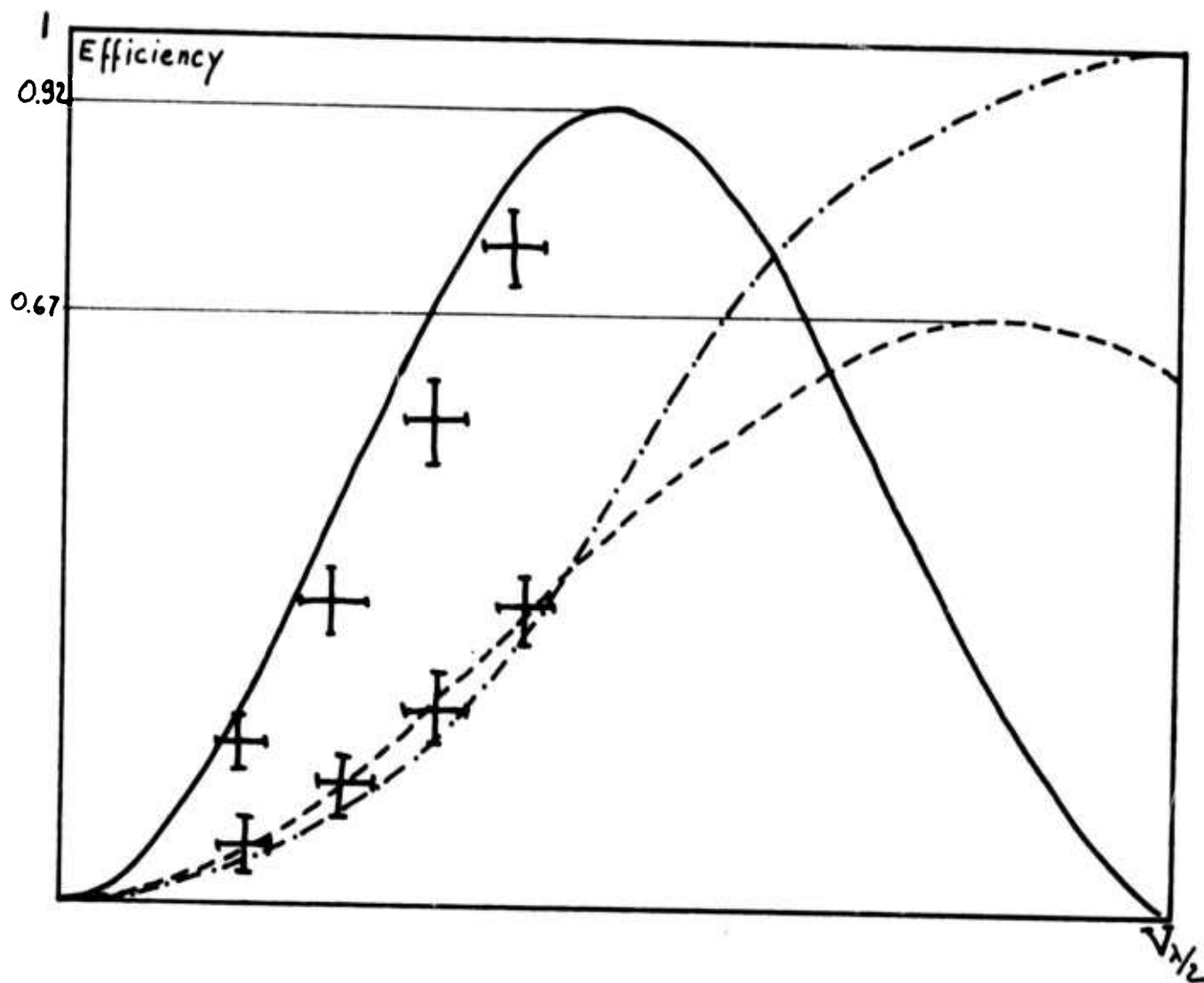
29

Fig. 3. Frequency conversion efficiency.

- - -   =   single pass two crystal set-up

———   =   double pass two crystal set-up

-·-·-   =   cubic crystal set-up

✚   =   experimental data

$$\mathcal{A}_{double \atop pass} = \frac{\sqrt{2}}{2} J_1\left(\delta\sqrt{2}\right) + J_1\left(\delta\right)$$

$$\approx \delta$$

$$\mathcal{A}_{single \atop pass} = \sqrt{2} J_1\left(\delta\frac{\sqrt{2}}{2}\right) \approx \frac{\delta}{2}$$

However, as far as the final efficiency and output stability are concerned, it does not seem that any substantial gain is obtained over the previous, single pass system. Due to the numerous surfaces along the path of the beam (i.e., linear polarizer, quarter wave plate, the two crystals, quartz windows), and due to the absorption by each of the components, the insertion loss is of the order of 50% for one passage through the frequency shifter. Hence, the double pass insertion loss counterbalances the theoretical gain in efficiency expected from the double pass configuration. Furthermore, this set-up wastes at least another half of the incoming light by letting the beam go twice through the beam splitter. Hence, the maximum efficiency in the double pass configuration should be at least four times larger than in the single pass in order to achieve the same power conversion from the initial frequency to the desired shifted frequency. We have shown that in the best case (small exciting voltage) it can be

31

at most four times as large, so that for the same applied voltage, less flux is obtained at the shifted frequency in the double pass configuration than in the single pass.

Another problem we have encountered in the double pass system is the feedback from reflection upon the output mirror of the laser. We have seen previously that if the beam of light is not propagating along the optic axes of the crystals, natural birefringence rapidly increases in value over induced birefringence and makes some of the light at the initial frequency appear in the output.

If we want to keep the spectral purity of the output very high, for example, with the energy being in the first order by more than a certain percentage, say 99.99%, so that the amplitude in the zeroth order is less than 1% of the amplitude of the first order, we have shown above that:

$$\frac{\pi}{\lambda}\left(n_e - n_o\right) d \, \varepsilon_{max}^2 \leq 0.01$$

where d is the thickness of the crystals and ε_{max} the maximum misalignment between the crystals' axes and the beam. With the actual characteristics of the set-up, we find that:

$$\varepsilon_{max} = 3 \times 10^{-2} \text{ radian}$$

Therefore, the beam has to come back as much as possible along the same way it came in. Care must be taken that the divergence of the beam from the laser does not exceed this limit, which is the case for the laser we are using. If the divergence of the laser beam was larger, one should match the beam to the crystals by putting the beam waist on the mirror as close as possible to the crystals.

When this alignment is done, much fluctuation can be noticed in the output of the frequency shifter, which can be explained by the fact that the mirror of the laser, the beam splitter and the final mirror act like a low re-flectance Fabry-Perot, internally modulated in frequency by the electro-optic crystals:

$$l = l_1 + l_2$$
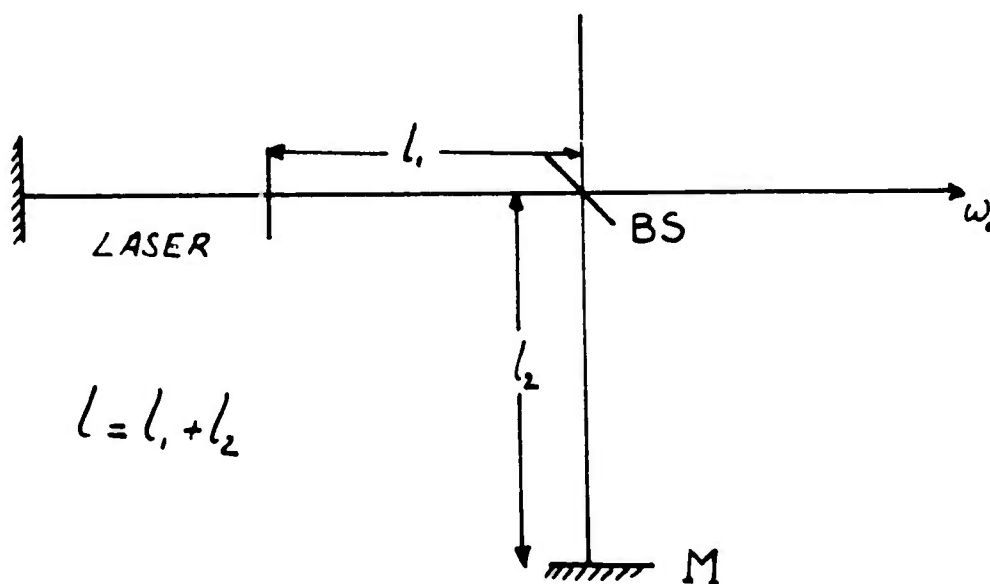
As seen previously, the frequency response of the double pass frequency shifter (without any feedback from the laser) to a quasi-monochromatic beam of light can be written as follows:

$$e^{i\omega_o t} \longrightarrow \sum_{-\infty}^{+\infty} \mathcal{A}_n e^{i(\omega_o + n\omega_m)t}$$

where the $\mathcal{A}_n$ coefficents are given on page 29. At each passage back through the system, each harmonic gives rise to an infinite series of outputs, and we find that the output beam after the beam splitter is made up of harmonics with the following amplitudes:

$$h_k = t \sum_{n=0}^{\infty} \rho^{2n+1} \sum_{p=-\infty}^{+\infty} \sum_q \sum_r \ldots \mathcal{A}_p \mathcal{A}_q \mathcal{A}_r \ldots e^{in\varphi}$$

where: h_k = amplitude of the kth harmonic.

t, ρ = amplitude transmittance and reflectance of the beam-splitter.

$$\varphi = \frac{2\pi}{\lambda} 2l$$

$$p + q + r + \ldots = k$$

For voltages lower than the quarter wave voltage of the crystals, the only non-negligible output for the double

34

pass frequency shifter without feedback is the first order, so that the amplitude of the optical field at the outset of the beam splitter is, taking the feedback into account:

$$\mathcal{A}_{TOTAL} = \rho t \mathcal{A}_1 e^{i(\omega_o + \omega_m)t} + \rho^3 t \mathcal{A}_1^2 e^{i[(\omega_o + 2\omega_m)t + \varphi]}$$
$$+ \rho^5 t \mathcal{A}_1^3 e^{i[(\omega_o + 3\omega_m)t + 2\varphi]} + \cdots$$

Any change in the distance l between the laser and the mirror M will modify the length of the cavity, hence φ , and modulate both the amplitude and phase of the output optical field represented by the phasor $\mathcal{A}_T$. In order to eliminate this problem, we have had to put an optical isolator (made up of a quarter wave plate followed by a linear polarizer), which prevents the light reflected from the output mirror of the laser from being re-injected into the frequency shifter.

III. A METHOD FOR OPTICALLY CORRECTING CRYSTAL AND GLASS LASER RODS

1. Review of Earlier Progress

As described in earlier contract reports, the sequence of steps in manufacturing an optical correction plate is as follows:

(1) The distortion to be corrected is determined by obtaining an interferogram of a wavefront which has been distorted by passage through the laser rod in question. This interferogram is essentially a contour map of the distorted wavefront, with contours spaced by a half wavelength, and also represents a contour map of the optical thickness of the desired correction plate (with high spots switched to low spots, etc).

(2) The correction plate is made by <u>grinding</u> a glass plate to match the contour map defined above, except that a scale factor M will be included; e.g. ten waves of distortion may be scaled up to an appreciable fraction of a millimeter so that the contouring can be accurately accomplished using an optical milling machine.

(3) Finally, the "magnified" correction plate is
     scaled back down to the proper magnitude by
     immersing the plate in a fluid whose refractive
     index very nearly matches that of the glass
     correction plate. An index mismatch of Δn
     produces a scale factor $M = 1/\Delta n$. This tech-
     nique of using near index-matching provides a
     number of additional advantages, the most
     important of which is that it does away with
     the necessity for optically polishing the
     correction plate since the surface roughness
     of the ground correction plate is scaled down
     by the same factor M . This prediction was
     confirmed experimentally at an early stage in
     this work.

To test the validity of this entire concept, we decided
to pick a piece of window glass, exhibiting about 20 fringes
of random deformation, and make a correction plate for it
in the manner described above. The sample to be corrected
was approximately 2 inches square. The interferogram was
photographed using a Twyman-Green interferometer with a
5461Å mercury light source. This photographic interferogram
was then digitized using an HP digitizer as described in

38

detail in earlier reports. The digitized data were then used to generate a paper tape which in turn was used to control an optical milling machine. This milling machine, which was simply a modified metal-working machine owned by the Frank Cooke Optical Company, could be controlled in cutting depth during constant feed by a paper tape reader. The transfer of data from the original digital form to the proper paper tape format proved to be a very lengthy and cumbersome procedure - but would of course be much simpler the next time around. The remainder of this report describes the operation of the tape-controlled milling machine in some detail, and assesses the quality of the correction plate which was made.

2. <u>Production of Scaled Correction Plates using a Tape-Controlled Milling Machine</u>

A. Machine control

As described earlier, by obtaining a digitized two-dimensional mapping of the interferogram we provide ourselves with a digital description of the distorted wavefront, and hence of the desired correction plate. The index matching scale factor M is then applied to generate the surface coordinates of the machined correction plate. In addition, in order to overcome the problem of back-lash

in the milling machine, the data were transferred to a tilted coordinate system (Fig. 4) so that the motion of the cutting tool was always in the same direction.
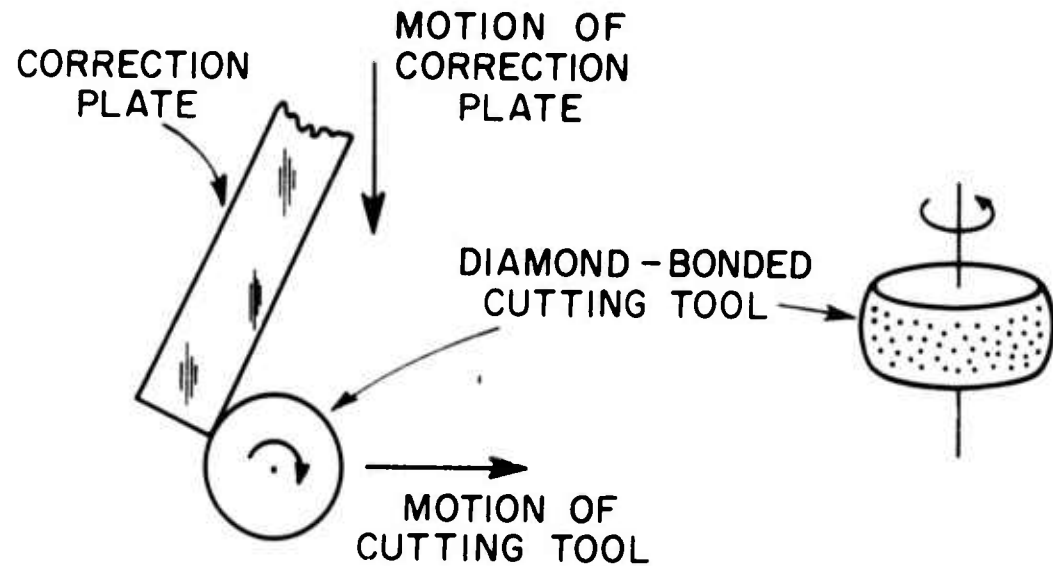

Fig. 4   Set-up for machining correction plate

Figure 5 shows the relative positions of the cutting tool and the glass plate at the beginning of a cutting "scan".
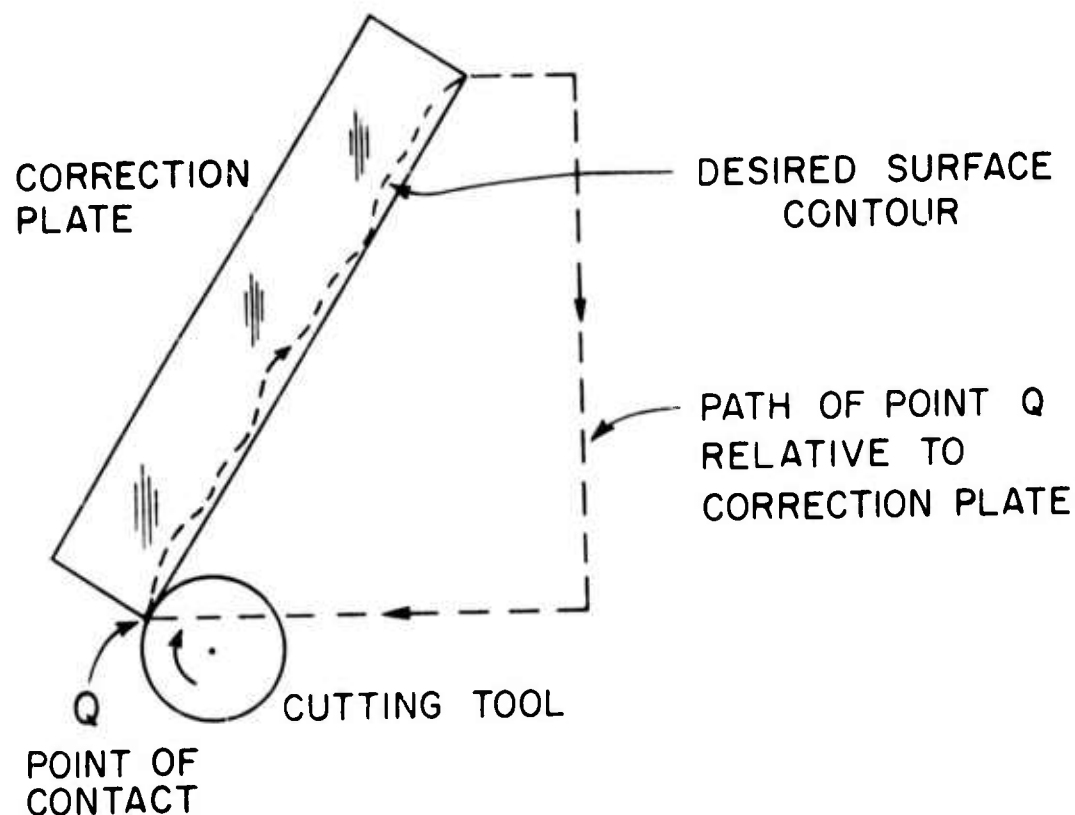
Fig. 5   Relative positions of cutting tool and glass plate
at the beginning of a cutting "scan"

As shown, the contour of the machined plate is actually

determined by the path of the point Q , which is the point

of contact between the tool and the glass plate. At the end

of a scan, the tool is returned to the starting position

and the correction plate is manually stepped in a direction

perpendicular to the plane of Fig. 5. Control of the machine

is then returned to the tape reader and the next adjacent

41

cutting scan is started. In producing the paper machine
control tapes we start by storing both the scaled-up and
transformed data sets, and also some control signals re-
quired for the milling machine operation. This information
was stored in the disc of an IBM 360, and then transferred
at a teletype terminal to paper tape. Since the code for-
mat of the teletype is the ASCII, we had to subsequently
convert it to the EIA format used by the milling machine.
This was done with the aid of an HP Computer Data Acquisition
System -- HP-2748A/Tape Reader, HP-2440A Analogue-Digital
Interface, and HP-7900A Disc Drive. As mentioned earlier,
this was an extremely awkward arrangement and could certain-
ly be circumvented in the future.

B. Design of the cutting wheel.

Although diamond-bonded glass-cutting tools can
now be made in virtually any shape and with any desired
size diamond grit, we ended up using one that Frank Cooke
had on hand. Following are some of the considerations in
designing the optimum shape tool. The tool is a section
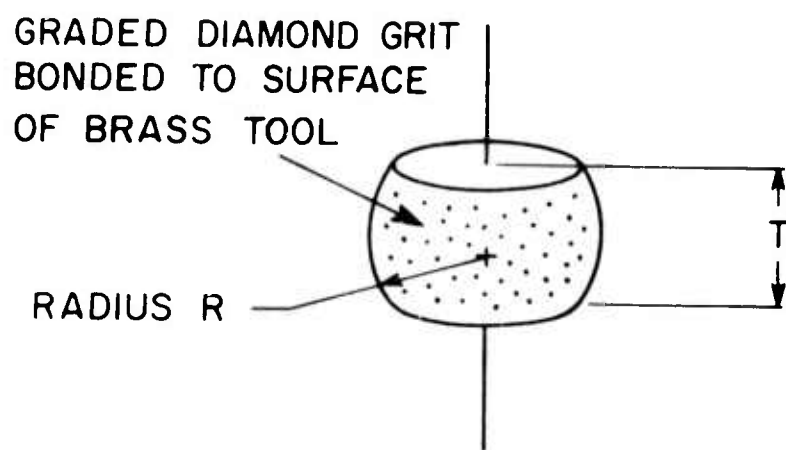of a sphere as shown in Fig. 6.

42

GRADED DIAMOND GRIT
BONDED TO SURFACE
OF BRASS TOOL

RADIUS R

T

Fig 6   Cutting tool

From the point of view of wear on the cutting tool, which

is far more subject to wear than a conventional metal-

cutting tool, the cutting surface area - and hence the tool

radius R - should be as large as possible. On the other

hand, fine control over the surface figure of the correction

plate requires a small radius tool. Fig. 7 shows a number

of parameters of the problem. In particular, the "residue"

is defined as the height of the cusp-shaped residual material

on the correction plate between cutting scans spaced by a

distance h . This residue must, of course, be small enough

to be reduced well below a wavelength after index matching.

It can easily be shown that the radius of the tool must
satisfy the following inequality in order to leave a
residue no larger than d , with a spacing between cutting
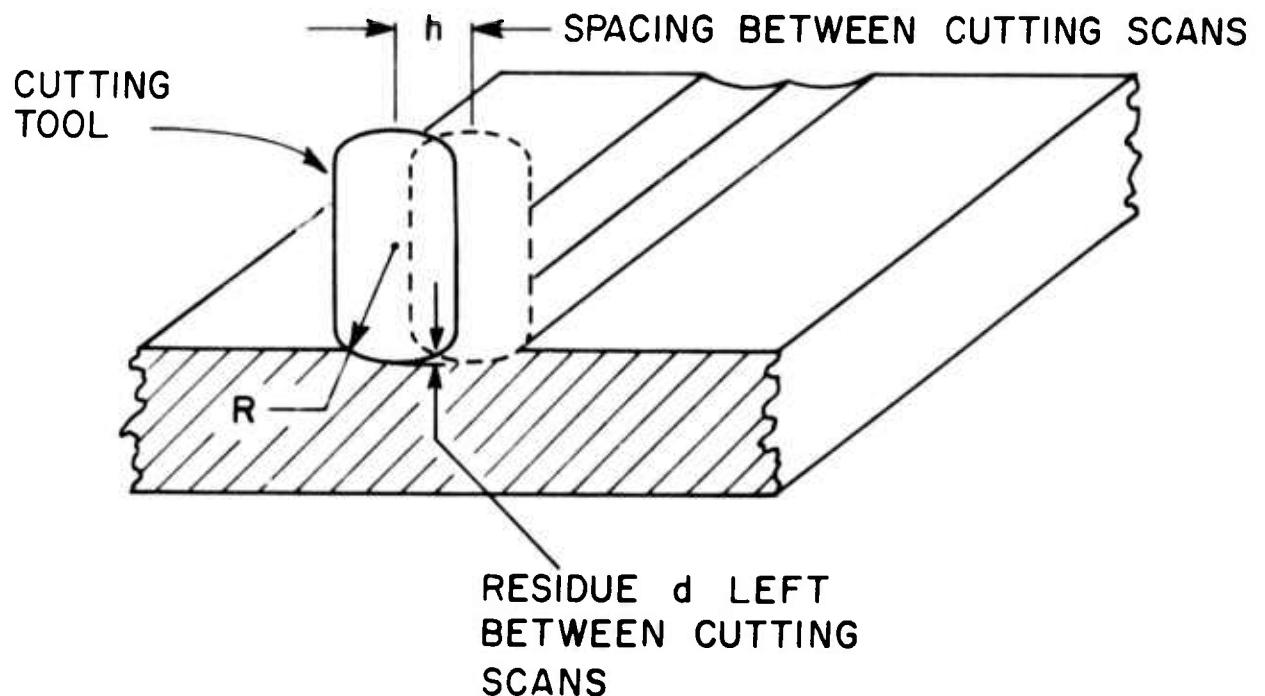scans of h .

$$R \; > \; h^2/8d$$

Fig. 7   Machining of the correction plate

The thickness, T , of the cutting wheel is not critical
but should certainly be large enough to ensure that the
tool will not vibrate or change shape during grinding.
Obviously, the tool thickness must be greater than the

44

spacing h between cutting scans.

Strictly speaking, the surface figure produced by cutting at the point of tangency between the tool and the correction plate is not identical with the locus of the cutting tool axis relative to the plate. This discrepancy could have been taken into account in producing the control tape, but was in fact small enough to safely neglect; the smaller the radius of the cutting tool, the smaller the discrepancy.

3. Assessment of Finished Correction Plate

The performance of the completed correction plate is illustrated in Figs. 8-11. A number of features are immediately apparent:

1. Because (i) we were unable to obtain the proper index matching fluid, and (ii) the residue, d , (see Fig. 7) was somewhat excessive due to the fact that we spaced the cutting scans too far apart in order to keep the machining costs down to a reasonable figure, the interference fringes in the index-matched correction plate have about a half-wavelength of deformation due to the residue. (This is why the fringes in Figs. 9-11 are "jagged".)
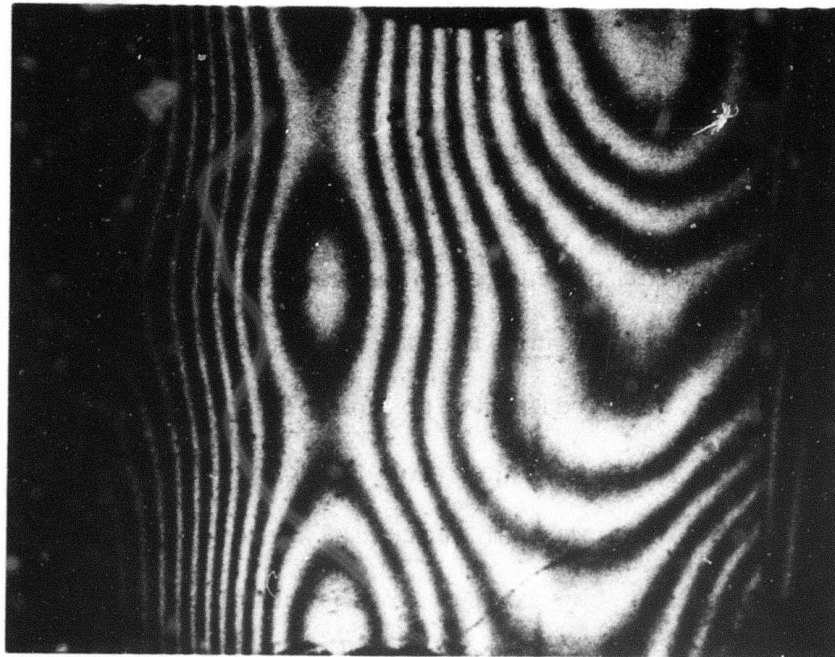
45

Fig. 8   Distorted wavefront to be corrected (2"x2");
         approximately 20 fringes (Twyman-Green interferogram)

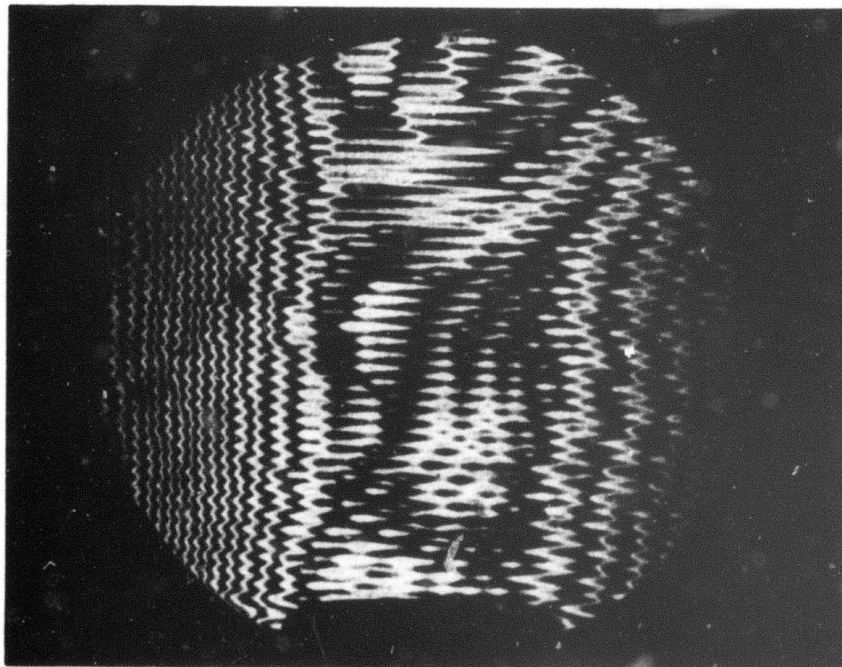
Fig. 9   Interferogram of imperfectly index-matched correction
         plate
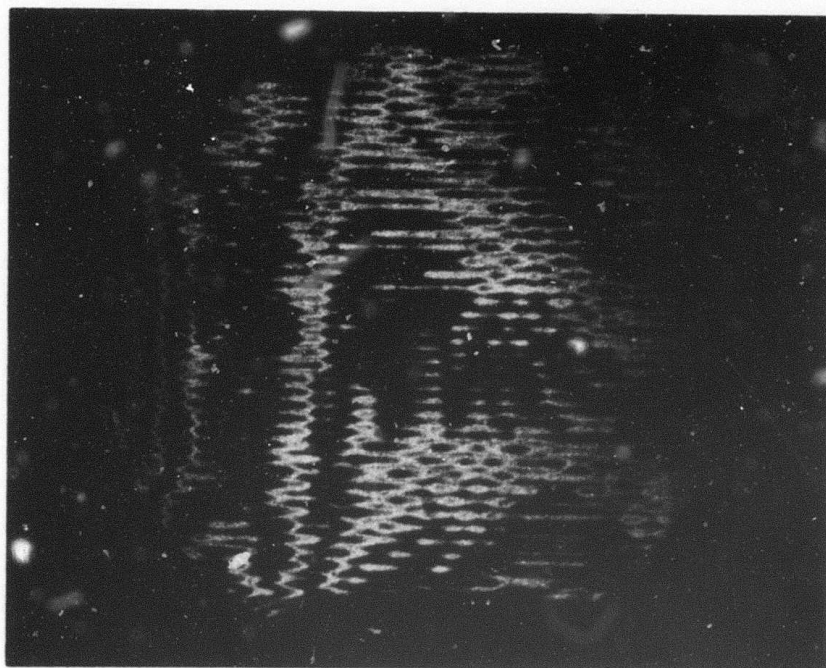
Fig. 10   Interferogram of corrected wavefront (approximately
           4 fringes)

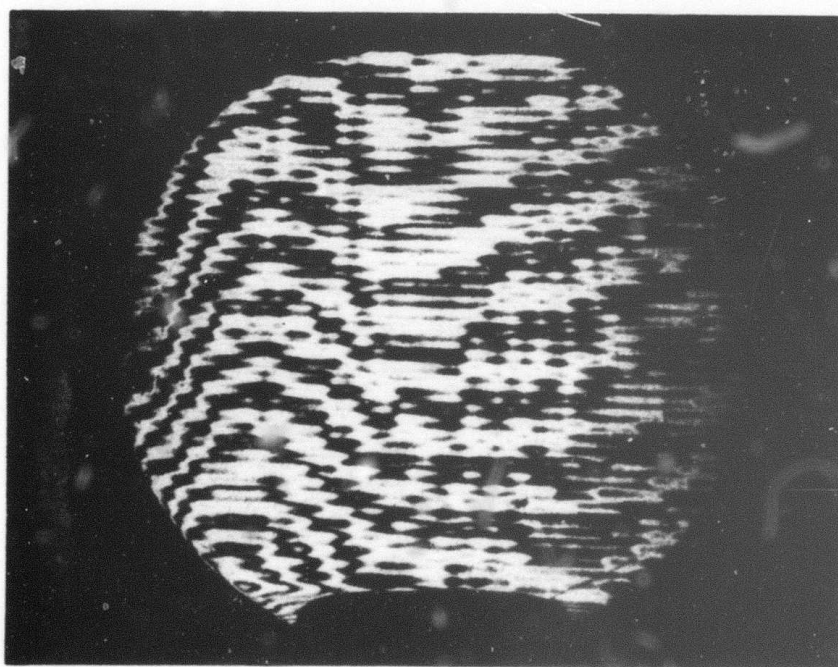

Fig. 11   Interferogram of imperfectly index-matched
           correction plate with reference wavefront slightly
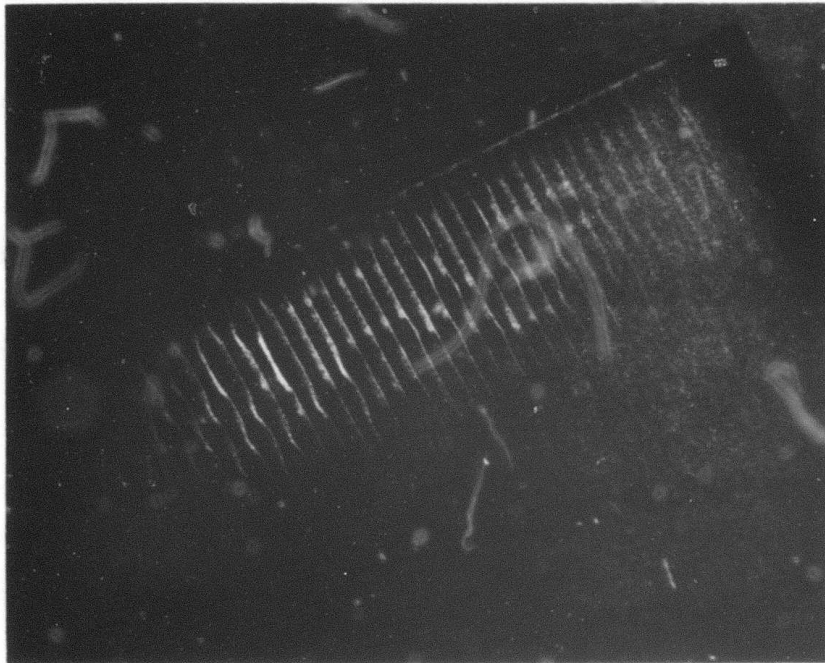   tilted.

47

Fig. 12   Photo of one edge of correction plate, showing
grooves and residue left by machining operation

2. The correction plate was successful: when placed in series with the plate to be corrected, a marked improvement in the quality of the transmitted wavefront was obtained. The uncorrected wavefront had about 20 fringes of deformation, while the corrected wavefront had just a couple of fringes. The improvement is particularly evident in Fig. 11, where some tilt was introduced in the interferometer to more clearly display the nature of the residual wavefront deformation.

We feel that this work, which consisted of (i) measuring the deformation to be corrected, (ii) digitizing the deformation information, (iii) preparing a paper tape to control an optical milling machine, (iv) machining a scaled-up correction plate, and (v) using the correction plate with the appropriate index-matching fluid to attempt to correct the original deformation, has been successful. We have clearly demonstrated the feasibility of this approach to correcting arbitrary wavefront deformations. With our current capability we could easily correct wavefront distortions of up to 50 wavelengths, to less than a wavelength. Our approach to this problem would be particularly well-suited

to the correction of large numbers of optical components, since initial programming, digitization, and optical machining can all be done relatively cheaply and routinely after the initial set-up.

APPENDIX

Program for Making a Correction Plate

```
/WATFOR
C       PROGRAM FOR MAKING A CORRECTION PLATE
C       GIN-HORNG CHEN, INSTITUTE OF OPTICS, UNIVERSITY OF ROCHESTER
        DIMENSION A(40,40),Y(40),XX(30),YY(101),XP(101),ZP(101,101)
        REAL*8 A,Y,DET
        LOGICAL*1 TAB/Z10/,MINUS/'-'/
        READ,NL,LL,DX,DY
C       NL=NUMBER OF SCAN LINES ACROSS INTERFEROGRAM
C       LL=NUMBER OF INTERPOLATED POINTS ALONG EACH SCAN LINE
C       DX=INTERVAL OF INTERPOLATION
C       DY=INTERVAL IN Y-DIRECTION BETWEEN SCAN LINES
        PRINT 101
  101 FORMAT(11X,'NL',11X,'LL',8X,'DX',16X,'DY')
        PRINT,NL,LL,DX,DY
        DO 102 L=1,LL
  102 XP(L)=DX*(L-1)
C
C       BEGIN MAPPING IN X-DIRECTION
        DO 100 M=1,NL
        READ,ND,(XX(K),K=1,ND),(YY(K),K=1,ND)
C       ND=NUMBER OF ORDERED DATA POINTS ALONG EACH SCAN LINE
C       XX(K)=X-COORDINATE OF KTH DATA POINT
C       YY(K)=Z-COORDINATE OF KTH DATA POINT
        DO 1 L=1,ND
    1 XX(L)=0.5*XX(L)
C       REDUCTION TO REAL VALUE OF XX(L) DUE TO ENLARGEMENT OF INTERFEROGRAM
        Y(1)=0.
        DO 2 K=1,ND
    2 Y(1)=Y(1)+YY(K)
        N=ND
        IF(N.GT.40) N=40
        DO 5 I=2,N
        Y(I)=0.
        DO 5 K=1,ND
        IF(I-35) 4,4,3
    3 IF(XX(K).LT.0.01) GO TO 5
    4 Y(I)=Y(I)+XX(K)**(I-1)*YY(K)
    5 CONTINUE
        A(1,1)=ND
        DO 13 J=2,N
        A(1,J)=0.
        A(J,N)=0.
        DO 11 K=1,ND
        IF(J-35) 7,7,6
    6 IF(XX(K).LT.0.1) GO TO 8
    7 A(1,J)=A(1,J)+XX(K)**(J-1)
    8 IF(J+N-36) 10,10,9
    9 IF(XX(K).LT.0.1) GO TO 11
   10 A(J,N)=A(J,N)+XX(K)**(J+N-2)
   11 CONTINUE
        JJ=J-1
        DO 12 I=1,JJ
        LI=1+I
        LJ=J-I
   12 A(LI,LJ)=A(1,J)
        IF(J.EQ.N) GO TO 14
        JJ=N-J
```

52

```
      DO 13 I=1,JJ
      KI=J+I
      KJ=N-I
   13 A(KI,KJ)=A(J,N)
   14 CALL DMATEQ(A,N,Y,DET)
C     NOW Y(I)=COEFFICIENTS OF POLYNOMIAL (LOW TO HIGH)
      ZP(M,1)=Y(1)
      DO 15 L=2,LL
      ZP(M,L)=Y(N)
      DO 15 I=2,N
   15 ZP(M,L)=ZP(M,L)*XP(L)+Y(N+1-I)
  100 CONTINUE
      DO 201 K=1,NL
  201 XX(K)=DY*(K-1)
      N=NL
      IF(N.GT.40) N=40
C
C     BEGIN MAPPING IN Y-DIRECTION
      DO 200 M=1,LL
      Y(1)=0.
      DO 21 K=1,NL
   21 Y(1)=Y(1)+ZP(K,M)
      DO 24 I=2,N
      Y(I)=0.
      DO 24 K=1,NL
      IF(I-35) 23,23,22
   22 IF(XX(K).LT.0.01) GO TO 24
   23 Y(I)=Y(I)+XX(K)**(I-1)*ZP(K,M)
   24 CONTINUE
      A(1,1)=NL
      DO 32 J=2,N
      A(1,J)=0.
      A(J,N)=0.
      DO 30 K=1,NL
      IF(J-35) 26,26,25
   25 IF(XX(K).LT.0.1) GO TO 27
   26 A(1,J)=A(1,J)+XX(K)**(J-1)
   27 IF(J+N-36) 29,29,28
   28 IF(XX(K).LT.0.1) GO TO 30
   29 A(J,N)=A(J,N)+XX(K)**(J+N-2)
   30 CONTINUE
      JJ=J-1
      DO 31 I=1,JJ
      LI=1+I
      LJ=J-I
   31 A(LI,LJ)=A(1,J)
      IF(J.EQ.N) GO TO 33
      JJ=N-J
      DO 32 I=1,JJ
      KI=J+I
      KJ=N-I
   32 A(KI,KJ)=A(J,N)
   33 CALL DMATEQ(A,N,Y,DET)
C     NOW Y(I)=COEFFICIENTS OF POLYNOMIAL (LOW TO HIGH)
C     WAVELENGTH= 5461 A ,  SCALING FACTOR M=200
C     ZP IN THE UNIT OF 1/10000 INCH
      ZP(1,M)=Y(1)*21.5
```

```
      DO 35 L=2,LL
      ZP(L,M)=Y(N)
      DO 34 I=2,N
   34 ZP(L,M)=ZP(L,M)*XP(L)+Y(N+1=I)
   35 ZP(L,M)=ZP(L,M)*21.5
C     ZP IN THE UNIT OF 1/10000 INCH
  200 CONTINUE
C
  500 FORMAT(I1,A1,I3)
  501 FORMAT(I2,A1,I3)
  502 FORMAT(I3,A1,I3)
  503 FORMAT(I4,A1,I3)
  600 FORMAT(I1,A1,A1,I4)
  601 FORMAT(I2,A1,A1,I4)
  602 FORMAT(I3,A1,A1,I4)
  603 FORMAT(I4,A1,A1,I4)
  505 FORMAT(I1,A1,I1,A1,I3)
  508 FORMAT(I4,A1,I2,A1,I3)
  509 FORMAT(I4,A1,I1,A1,I3)
  510 FORMAT(I3,A1,I2,A1,I3)
  511 FORMAT(I3,A1,I1,A1,I3)
  512 FORMAT(I2,A1,I2,A1,I3)
  513 FORMAT(I2,A1,I1,A1,I3)
  514 FORMAT(I1,A1,I2,A1,I3)
  515 FORMAT(I1,A1,A1,A1,I5,A1,A1,A1,I2)
  516 FORMAT(I2,A1,A1,A1,I5,A1,A1,A1,I2)
  517 FORMAT(I3,A1,A1,A1,I5,A1,A1,A1,I2)
  518 FORMAT(I4,A1,A1,A1,I5,A1,A1,A1,I2)
  520 FORMAT(I1,A1,A1,I4,A1,A1,A1,A1,I1,I1,I2)
  521 FORMAT(I2,A1,A1,I4,A1,A1,A1,A1,I1,I1,I2)
  522 FORMAT(I3,A1,A1,I4,A1,A1,A1,A1,I1,I1,I2)
  523 FORMAT(I4,A1,A1,I4,A1,A1,A1,A1,I1,I1,I2)
C
      NOX=600
      NOY=5100
C     NOX  NOY  FOR TRANSLATION
      S3=0.05234
      C3=0.99863
C     S3  C3  FOR TRANSFORMATION
      IH=55
      IS=0
      IT=6
C     IH  IS  IT  FOR CONTROL SIGNALS
      NO=0
C     NO IS THE SEQUENCE NUMBER
      DO 499 I=1,48
C
C     TRANSFORMATION AND TRANSLATION
      DO 406 J=1,LL
      YY(J)=NOY+XP(J)*10000.*C3+ZP(I,J)*S3
      IY=YY(J)
      IF(YY(J)-IY-0.5) 401,401,402
  401 YY(J)=IY
      GO TO 403
  402 YY(J)=IY+1
  403 ZP(I,J)=NOX-(XP(J)*10000.*(-S3)+ZP(I,J)*C3)
      IZ=ZP(I,J)
```

54

```
      IF(ZP(I,J)-IZ-0.5) 404,404,405
404   ZP(I,J)=IZ
      GO TO 406
405   ZP(I,J)=IZ+1
406   CONTINUE
C

      NO=NO+1
      IX=ZP(I,1)
      IF(NO.GT.999) GO TO 413
      IF(NO.GT.99) GO TO 412
      IF(NO.GT.9) GO TO 411
      WRITE(10,500) NO,TAB,IX
      GO TO 414
411   WRITE(10,501) NO,TAB,IX
      GO TO 414
412   WRITE(10,502) NO,TAB,IX
      GO TO 414
413   WRITE(10,503) NO,TAB,IX
414   NO=NO+1
      IY=YY(1)
      IF(NO.GT.999)GO TO 417
      IF(NO.GT.99)GO TO 416
      IF(NO.GT.9)GO TO 415
      WRITE(10,600)NO,TAB,TAB,IY
      GO TO 419
415   WRITE(10,601)NO,TAB,TAB,IY
      GO TO 419
416   WRITE(10,602)NO,TAB,TAB,IY
      GO TO 419
417   WRITE(10,603)NO,TAB,TAB,IY
419   DO 430 J=2,LL
      NO=NO+1
      IX=ZP(I,J)-ZP(I,J-1)
      IY=YY(J)-YY(J-1)
      IF(NO.GT.999.AND.IX.GT.0) GO TO 423
      IF(NO.GT.999.AND.IX.EQ.0) GO TO 424
      IF(NO.GT.99.AND.IX.GT.0) GO TO 425
      IF(NO.GT.99.AND.IX.EQ.0) GO TO 426
      IF(NO.GT.9.AND.IX.GT.0) GO TO 427
      IF(NO.GT.9.AND.IX.EQ.0) GO TO 428
      IF(IX.GT.0) GO TO 429
      WRITE(10,505) NO,TAB,IX,TAB,IY
      GO TO 430
423   WRITE(10,508) NO,TAB,IX,TAB,IY
      GO TO 430
424   WRITE(10,509) NO,TAB,IX,TAB,IY
      GO TO 430
425   WRITE(10,510) NO,TAB,IX,TAB,IY
      GO TO 430
426   WRITE(10,511) NO,TAB,IX,TAB,IY
      GO TO 430
427   WRITE(10,512) NO,TAB,IX,TAB,IY
      GO TO 430
428   WRITE(10,513) NO,TAB,IX,TAB,IY
      GO TO 430
429   WRITE(10,514) NO,TAB,IX,TAB,IY
430   CONTINUE
```

```
      NO=NO+1
      IY=YY(LL)
      IF(NO.GT.999) GO TO 443
      IF(NO.GT.99) GO TO 442
      IF(NO.GT.9) GO TO 441
      WRITE(10,515) NO,TAB,TAB,MINUS,IY,TAB,TAB,TAB,IH
      GO TO 450
441   WRITE(10,516) NO,TAB,TAB,MINUS,IY,TAB,TAB,TAB,IH
      GO TO 450
442   WRITE(10,517) NO,TAB,TAB,MINUS,IY,TAB,TAB,TAB,IH
      GO TO 450
443   WRITE(10,518) NO,TAB,TAB,MINUS,IY,TAB,TAB,TAB,IH
450   NO=NO+1
      IX=ZP(I,LL)
      IF(I.EQ.48)IT=2
      IF(NO.GT.999) GO TO 453
      IF(NO.GT.99) GO TO 452
      IF(NO.GT.9) GO TO 451
      WRITE(10,520) NO,TAB,MINUS,IX,TAB,TAB,TAB,TAB,IS,IT,IH
      GO TO 460
451   WRITE(10,521) NO,TAB,MINUS,IX,TAB,TAB,TAB,TAB,IS,IT,IH
      GO TO 460
452   WRITE(10,522) NO,TAB,MINUS,IX,TAB,TAB,TAB,TAB,IS,IT,IH
      GO TO 460
453   WRITE(10,523) NO,TAB,MINUS,IX,TAB,TAB,TAB,TAB,IS,IT,IH
460   CONTINUE
499   CONTINUE
      STOP
      END
```

REFERENCES

1. R. Crane, "Interference Phase Measurement", Appl. Opt., 8, 538-542, (March 1969).

2. G. E. Sommargren and B. J. Thompson, "Linear Phase Microscopy", Appl. Opt., 12, 2130-2138, (Sept. 1973).

3. C. F. Buhrer, L. R. Bloom and D. H. Baird, "Electro-optic Light Modulation with Cubic Crystals", Appl. Opt., 2, 839, (August 1963).

4. J. P. Campbell and W. H. Steier, "Rotating Waveplate Optical Frequency Shifting in Lithium Niobate", IEEE Journal of Q. E., QE-7, No. 9, (Sept. 1971).

5. I. P. Kaminow and E. H. Turner, "Electro-optic Light Modulators", Appl. Opt., 5, 1612, (Oct. 1966).

6. C. G. B. Garrett and M. A. Duguay, "Theory of the Optical Frequency Translator", App. Phys. Let., 9, 374, (Nov. 1966).

7. M. Gottlieb and M. Garbuny, "Analysis of the Spectrum of a Laser Beam Modulated by a Periodic Electro-optic Doppler Shift", Appl. Opt, 7, 2238, (Nov. 1968).